



## Modelling the thermal quenching mechanism in quartz based on time-resolved optically stimulated luminescence

V. Pagonis<sup>a,\*</sup>, C. Ankjærgaard<sup>b</sup>, A.S. Murray<sup>c</sup>, M. Jain<sup>c</sup>, R. Chen<sup>d</sup>, J. Lawless<sup>e</sup>, S. Greilich<sup>b</sup>

<sup>a</sup> McDaniel College, Physics Department, Westminster, MD 21157, USA

<sup>b</sup> Radiation Research Division, Risø National Laboratory for Sustainable Energy, Technical University of Denmark, DK-4000 Roskilde, Denmark

<sup>c</sup> Nordic Laboratory for Luminescence Dating, Department of Earth Science, Aarhus University, Risø DTU, DK-4000 Roskilde, Denmark

<sup>d</sup> Raymond and Beverly Sackler School of Physics and Astronomy, Tel-Aviv University, Tel-Aviv 69978, Israel

<sup>e</sup> Redwood Scientific Inc., Pacifica, CA 94044, USA

### ARTICLE INFO

#### Article history:

Received 31 August 2009

Received in revised form

16 December 2009

Accepted 18 December 2009

Available online 29 December 2009

#### Keywords:

Time resolved luminescence

Optically stimulated luminescence

Pulsed OSL

Thermoluminescence

Quartz

Luminescence lifetimes

Kinetic rate equations

Kinetic model

### ABSTRACT

This paper presents a new numerical model for thermal quenching in quartz, based on the previously suggested Mott–Seitz mechanism. In the model electrons from a dosimetric trap are raised by optical or thermal stimulation into the conduction band, followed by an electronic transition from the conduction band into an excited state of the recombination center. Subsequently electrons in this excited state undergo either a direct radiative transition into a recombination center, or a competing thermally assisted non-radiative process into the ground state of the recombination center. As the temperature of the sample is increased, more electrons are removed from the excited state via the non-radiative pathway. This reduction in the number of available electrons leads to both a decrease of the intensity of the luminescence signal and to a simultaneous decrease of the luminescence lifetime. Several simulations are carried out of time-resolved optically stimulated luminescence (TR-OSL) experiments, in which the temperature dependence of luminescence lifetimes in quartz is studied as a function of the stimulation temperature. Good quantitative agreement is found between the simulation results and new experimental data obtained using a single-aliquot procedure on a sedimentary quartz sample.

© 2009 Elsevier B.V. All rights reserved.

### 1. Introduction

The phenomenon of thermal quenching of the stimulated luminescence in quartz has been well-known for several decades (see for example, Bøtter-Jensen et al. [1], p. 44, and references therein). Thermal quenching manifests itself as a reduction of the measured luminescence intensity from quartz as the sample temperature is raised, and has been observed in both thermoluminescence (TL) and optically stimulated luminescence (OSL) experiments on quartz ([2–4]). A model has been suggested previously for explaining thermal quenching in quartz, known as the Mott–Seitz mechanism (see for example [1,5,6], and references therein). Although the Mott–Seitz mechanism has been discussed extensively in the TL/OSL literature for quartz, to the best of our knowledge there has been no numerical modeling of the kinetic processes involved.

In addition to the well-known effects on the TL and OSL intensities, thermal quenching also affects the apparent luminescence lifetimes in quartz (and other dosimetric materials, see for example Ref. [7]). Over the past decade, extensive time-resolved

OSL (TR-OSL) measurements have been carried out using samples of both quartz and feldspars, reflecting the importance of these materials in dating and retrospective dosimetry ([8–14]). During TR-OSL measurements, the stimulation is carried out with a brief light pulse and photons are recorded based on their arrival at the luminescence detector with respect to the light pulse. Summing signals from several pulses gives rise to the typical TR-OSL curve that shows the buildup of luminescence during the pulse and the subsequent decrease after the pulse on ns to ms time scales, depending on the processes involved. The decaying signal immediately following any light pulse can be analyzed using the linear sum of exponential decays, and can therefore be characterized using decay constant(s) or lifetime(s). The main advantage of TR-OSL over CW-OSL is that it allows study of such recombination and/or relaxation pathways.

Several researchers have studied the temperature dependence of luminescence lifetimes and luminescence intensity from time-resolved luminescence spectra in quartz (see for example, [15–19] and references therein). The luminescence lifetimes for unannealed sedimentary quartz typically are found to remain constant at  $\sim 42 \mu\text{s}$  for stimulation temperatures between 20 and 100 °C, and then to decrease continuously to  $\sim 8 \mu\text{s}$  at 200 °C.

The purpose of this paper is to present a new kinetic model for thermal quenching in quartz based on the Mott–Seitz mechanism.

\* Corresponding author. Tel.: +1 410 857 2481; fax: +1 410 386 4624.

E-mail address: [vpagonis@mcDaniel.edu](mailto:vpagonis@mcDaniel.edu) (V. Pagonis).

In this model all recombination transitions are localized within the recombination center (in contrast to a delocalized model, where all charge transitions take place to or from the conduction and valence bands—e.g. Ref. [6]).

Several simulations of typical TR-OSL experiments are carried out using the model, and the results are compared to new measurements of the luminescence lifetimes and luminescence intensity of a sedimentary quartz sample as a function of the stimulation temperature.

## 2. Experimental

In the experimental work presented here, sedimentary quartz (sample WIDG8; Ref. [20]) with grain size 90–125  $\mu\text{m}$  has been used. The quartz were extracted from the sample by sieving, heavy liquid separation and HF treatment; the absence of significant feldspar contamination was confirmed by tests using IR stimulation. Sample measurements were carried out on a Risø TL/OSL-20 reader with an integrated pulsing option to control the stimulation LEDs, and with a photon timer attachment with a channel width of 100 ps to record the TR-OSL data ([21]). Blue light stimulation was performed with an LED array emitting at  $470 \pm 30$  nm, and delivering  $50 \text{ mW cm}^{-2}$  CW stimulation at the sample position; a 7.5 mm thick Hoya U340 filter was used. The duration of both the on- and off-pulse widths can be set independently to between 0.2  $\mu\text{s}$  and 9.9 s (on-time) and between 0.6  $\mu\text{s}$  and 9.9 s (off-time), although the pulse shape deteriorates for pulse widths  $< 6 \mu\text{s}$ . During a pulsed measurement, the photon timer records the time of arrival of photons detected during and after the pulse (relative to the beginning of the pulse).

In the measurements, a single aliquot of the quartz sample WIDG8 was optically bleached with blue light for 100 s at 260  $^{\circ}\text{C}$  in order to empty all optically active traps, and was subsequently given a beta dose of 5 Gy. It was then preheated for 10 s at 260  $^{\circ}\text{C}$  and the TR-OSL was measured by repeatedly turning the optical stimulation ON for 50  $\mu\text{s}$  and OFF for 500  $\mu\text{s}$ . This was followed by an optical bleach for 100 s at 260  $^{\circ}\text{C}$ . The whole process was repeated for higher stimulation temperatures, from 20 to 320  $^{\circ}\text{C}$  in steps of 20  $^{\circ}\text{C}$ . Recycling measurements were done for the stimulation temperatures 40, 100, 200, and 300  $^{\circ}\text{C}$ .

## 3. The Mott–Seitz mechanism of thermal quenching in quartz

The principles behind the Mott and Seitz mechanism of thermal quenching in quartz have been summarized previously, for example in Bøtter-Jensen et al. [1], page 44. The Mott–Seitz mechanism is usually shown schematically using a configurational diagram as in Fig. 1a, and consists of an excited state of the recombination center and the corresponding ground state. In this mechanism, electrons are captured into an excited state of the recombination center, from which they can undergo either one of two competing transitions. The first transition is a direct radiative recombination route resulting in the emission of light and is shown as a vertical arrow in Fig. 1a. The second route is an indirect thermally assisted non-radiative transition into the ground state of the recombination center; the activation energy  $W$  for this non-radiative process is also shown in Fig. 1a. The energy given up in the non-radiative recombination is absorbed by the crystal as heat, rather than being emitted as photons. One of the main assumptions of the Mott–Seitz mechanism is that the radiative and non-radiative processes compete within the confines of the recombination center, hence they are referred to as localized transitions.

During TR-OSL experiments a brief exposure to stimulating light (a light pulse) raises a small number of electrons from the electron trap into the conduction band (CB); some of these electrons are then trapped by the excited state of the recombination center (RC). Electrons trapped in this excited state may then relax to the ground state of the RC through a direct radiative transition (resulting in emission of a photon) or through a non-radiative transition (in which the relaxation energy increases the thermally induced vibrations of the lattice, Fig. 1a). In the approach first described by Mott ([22,23]), the probability of the non-radiative process,  $A_{NR}$ , is assumed to have a temperature dependent scaling described by a Boltzmann factor of the form  $\exp(-W/k_B T)$ , where  $W$  is the activation energy,  $T$  temperature and  $k_B$  Boltzmann's constant, while the radiative probability  $A_R$  is assumed to be a constant independent of temperature. The constants  $A_R$  and  $A_{NR}$  have dimensions of  $\text{s}^{-1}$ . Thus, the experimentally observed luminescence will be proportional to the luminescence efficiency ratio  $\eta(T)$  defined by the relative probabilities of radiative and non-radiative transitions

$$\eta(T) = \frac{A_R}{A_R + A_{NR} \exp(-W/k_B T)} = \frac{1}{1 + \frac{A_{NR}}{A_R} \exp(-W/k_B T)}. \quad (1)$$

Experimentally it has been found that the CW-OSL or the 325  $^{\circ}\text{C}$  TL peak intensity from quartz samples follow a very similar expression to Eq. (1) with the empirical form:

$$I(T) = \frac{I_0}{1 + C \exp(-W/k_B T)}, \quad (2)$$

where  $I_0$  is the luminescence intensity at low temperatures and  $C$  a dimensionless constant ([19], Eq. (7); [20,21]). As the temperature of the quartz sample is increased during stimulation, the experimentally measured luminescence intensity  $I(T)$  decreases with temperature according to Eq. (2). This empirically observed form is similar to the expression derived on the basis of Mott–Seitz mechanism i.e. Eq. (1). By comparison of the empirical expression (2) with the luminescence efficiency expression (1), the dimensionless empirical constant  $C$  appearing in Eq. (2) can be interpreted as the ratio of the non-radiative and radiative probabilities  $A_{NR}/A_R$ .

However, in order to test whether the Mott–Seitz mechanism could be responsible for thermal quenching in quartz, one should be able to make estimates of transition probabilities as a function of temperature; these estimates are unfortunately not possible in CW-OSL or TL measurements. However, the analysis of time-resolved OSL signals offers such a possibility. Recently Chithambo ([19], Eq. 5) has shown that the luminescence lifetime ( $\tau$ ) derived from the TR-OSL signals of quartz samples also shows a similar temperature dependence

$$\tau = \frac{\tau_0}{1 + C \exp(-W/k_B T)}, \quad (3)$$

where  $\tau_0 = 42 \mu\text{s}$  is the experimentally-observed lifetime for the radiative process in unannealed quartz at low temperatures. As the temperature  $T$  of the sample is increased during the optical stimulation the lifetime  $\tau(T)$  of the electrons in the excited state decreases according to Eq. (3).

A good agreement between Eq. 2 (or (3)) and the TR-OSL data thus lends support to the Mott–Seitz model as possible explanation for thermal quenching in quartz. To our knowledge a mathematical implementation of this model has not been undertaken before; the schematic approach in Fig. 1a is not based on a detailed numerical model involving electronic transitions between energy states within the recombination center. The purpose of this paper is to develop and test such a kinetic model.

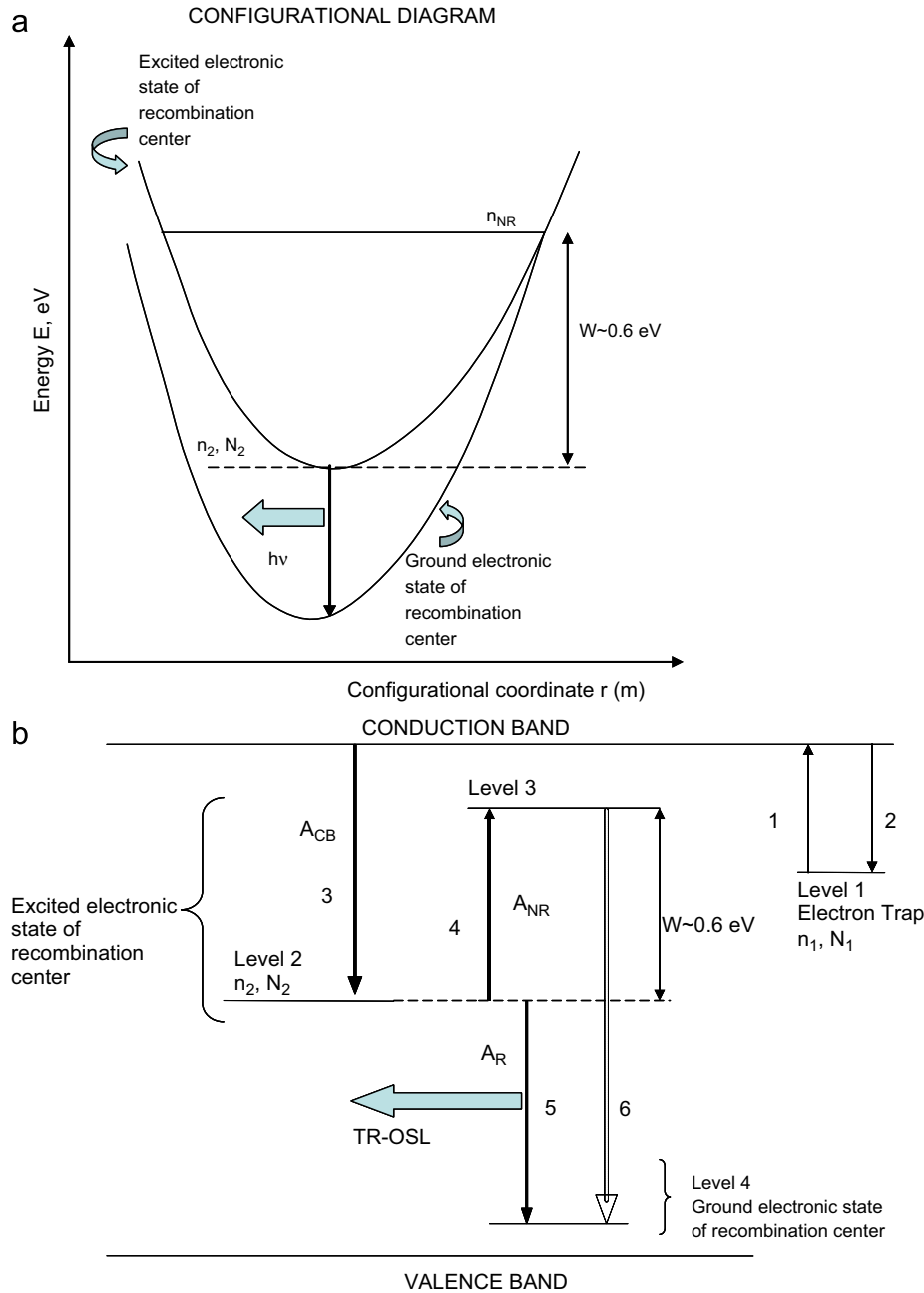


**Fig. 1.** (a) The configurational diagram outlining the Mott–Seitz mechanism in quartz and (b) schematic diagram of the thermal quenching model for quartz, which contains a dosimetric trap (level 1), two excited states within the radiative recombination center (levels 2 and 3), and the corresponding ground state (level 4). The various transitions shown and the parameters used in the model are described in the text.

#### 4. A kinetic model for thermal quenching in quartz

Fig. 1b shows the energy level diagram in a simple new model based on the Mott–Seitz mechanism, with the corresponding electronic transitions taking place during a typical TR-OSL experiment. The model consists of a dosimetric trap shown as level 1, and three levels labeled 2–4 representing energy states within the recombination center. During the transition labeled 1 in Fig. 1, electrons from a dosimetric trap are raised by optical stimulation into the CB, with some of these electrons being retrapped as shown in transition 2 with a probability  $A_n$ . Transition 3 corresponds to an electronic transition from the CB into the excited state located below the conduction band with probability  $A_{CB}$ . Transition 5 indicates the direct radiative

transition from the excited level into the ground electronic state with probability  $A_R$ , and transition 4 indicates the competing thermally assisted route. The probability for this competing thermally assisted process is given by a Boltzmann factor of the form  $A_{NR} \exp(-W/k_B T)$  where  $W$  represents the activation energy for this process and  $A_{NR}$  a constant representing the non-radiative transition probability (i.e. the probability of non-radiative transition at infinite temperature). Transition 6 denotes the non-radiative process into the ground state, the dashed arrow in the Fig. 1b indicating that it is not a discrete energy loss but rather a continuous energy loss resulting in heat. The details of the non-radiative process of releasing energy in the model are not important; what is important in determining the thermal quenching effects is the ratio of the non-radiative and radiative

probabilities  $A_{NR}/A_R$ , or the constant  $C$  defined from empirical observations, and the value of the thermal activation energy  $W$ .

The competing transitions 4 and 5 in Fig. 1b form the basis of our description of the thermal quenching process in quartz and are the causes of two simultaneous effects. As the temperature of the sample is increased, electrons are removed from the excited state according to the Boltzmann factor described above. This reduction leads to both a decrease of the intensity of the luminescence signal and to a simultaneous apparent decrease of the luminescence lifetime.

Several experiments ([2–4,16]) have reported a range of values of the constants  $C$ ,  $W$  appearing in Eqs. (1) through (3). Typical ranges for the numerical values for these constants in quartz are  $W=0.5–0.8$  eV and  $C=10^6–10^8$  (see for example, Chithambo [16], Table 1 for a tabulation of several results). The parameters used in the model are defined as follows;  $N_1$  is the concentration of electrons in the dosimetric traps ( $m^{-3}$ ),  $n_1$  the corresponding concentration of trapped electrons ( $m^{-3}$ ),  $N_2$  and  $n_2$  the concentrations of electron traps and filled traps correspondingly in the excited level 2 of the recombination center ( $m^{-3}$ ),  $W=0.64$  eV the activation energy for the thermally assisted process (eV),  $A_n$  the conduction band to electron trap transition probability coefficient ( $m^3 s^{-1}$ ),  $A_R$  and  $A_{NR}$  the radiative and non-radiative transition probability coefficients ( $s^{-1}$ ) and  $A_{CB}$  the transition probability coefficient ( $m^3 s^{-1}$ ) for the conduction band to excited state transition. The parameter  $n_c$  represents the instantaneous concentration of electrons in the conduction band ( $m^{-3}$ ) and  $P$  denotes the probability of optical excitation of electrons from the dosimetric trap ( $s^{-1}$ ).

The equations used in the model are as follows:

$$\frac{dn_1}{dt} = n_c(N_1 - n_1)A_n - n_1P, \quad (4)$$

$$\frac{dn_c}{dt} = -n_c(N_1 - n_1)A_n + n_1P - A_{CB}n_c(N_2 - n_2), \quad (5)$$

$$\frac{dn_2}{dt} = A_{CB}n_c(N_2 - n_2) - A_Rn_2 - n_2A_{NR} \exp(-W/k_B T). \quad (6)$$

The instantaneous luminescence  $I(t)$  resulting from the radiative transition is defined as

$$I(t) = A_R n_2. \quad (7)$$

It is noted that transitions 4, 5 and 6 in Fig. 1a are of a localized nature, while transition 3 involves electrons in the CB and hence is delocalized. The difference in the nature of these transitions can also be seen in their mathematical forms in Eqs. (4–7). The term  $A_{CB}n_c(N_2 - n_2)$  in Eqs. (5) and (6) expresses the fact that there are  $N_2 - n_2$  empty electronic states available for electrons in the CB; these states are excited states of the recombination center, in agreement with the general assumptions of the Mott–Seitz mechanism of thermal quenching.

The values of the parameters used in the model are as follows:  $A_n = 5 \times 10^{-14} m^3 s^{-1}$ ,  $A_R = 1/42 \mu s = 2.38 \times 10^4 s^{-1}$ ,  $A_{CB} = 10^{-8} m^3 s^{-1}$ ,  $P = 0.2 s^{-1}$ ,  $N_1 = 10^{14} m^{-3}$ ,  $N_2 = 10^{14} m^{-3}$ .

In the absence of any experimental evidence to the contrary, we will make the assumption that the conduction band empties much faster than the luminescence process in the recombination center which is assumed to take place with the experimentally observed luminescence lifetime of  $\sim 42 \mu s$ . We therefore choose the values of the delocalized transition probability  $A_{CB}$  and of the concentration  $N_2$  such that the conduction band empties very quickly when the stimulating light is switched off, on a time scale of  $\sim 1 \mu s$ . Note that the chosen values of  $A_{CB}$  and  $N_2$  are about 1 and 3 orders of magnitude higher than those used by Bailey [6], respectively. Without such an increase in either the transition probability and/or the value of  $N_2$ , it is not possible to empty the conduction band

sufficiently quickly to explain the experimental TR-OSL results using a model in which the recombination center is thermally quenched. The value of the radiative transition probability  $A_R = 1/42 \mu s = 2.38 \times 10^4 s^{-1}$  is taken from experimentally measured luminescence lifetime of  $\tau = 42 \mu s$  at room temperature ([13], [19]). The value of the non-radiative probability  $A_{NR}$  was treated as an adjustable parameter within the model, and is adjusted to obtain the best possible fits to the experimental data. The initial conditions for the different concentrations are taken as:  $n_1(0) = 9 \times 10^{13} m^{-3}$ ,  $n_2(0) = 0$ ,  $n_c(0) = 0$ .

The results of the simulation were tested by varying the parameters in the model within a physically reasonable range of values. Not surprisingly given the choice of a conduction band lifetime very much less than the lifetime of the excited state of the recombination center, it was found that the results remained unchanged when the parameters were varied within the following ranges of values:

$$A_n = 5 \times 10^{-12} - 5 \times 10^{-16} m^3 s^{-1}, A_{CB} = 10^{-5} - 10^{-8} m^3 s^{-1}, \\ N_1 = 10^{10} - 10^{17} m^{-3}, N_2 = 10^{13} - 10^{16} m^{-3}, \\ n_1(0) = 9 \times 10^{10} - 9 \times 10^{13} m^{-3}.$$

The results of the simulation only depended significantly on the values of the radiative and non-radiative probabilities  $A_R$  and  $A_{NR}$  used in the model. These dependencies of the results on the parameters make physical sense, since the Mott–Seitz mechanism is primarily an internal competition mechanism within the recombination center, and should not depend critically on the values of the external parameters in the model.

Thus, TR-OSL gives us a very useful insight into the lower limits of these parameter values.

## 5. Simulation of a typical TR-OSL experiment using the new model

We have simulated a typical TR-OSL experiment in which the optical stimulation is initially ON for 200  $\mu s$  and is subsequently turned OFF for the same amount of time. Fig. 2 shows the results of this simulation using the model in Fig. 1b, and with the parameters listed in the previous section. The decaying part of the signal in Fig. 2 has been fitted to a decaying exponential, while the rising part of the signal in the same figure is fitted to a saturating exponential function. The fits are shown as solid lines through the simulated data, and they yield almost identical luminescence lifetimes with values  $\tau_{rise} = (41.8 \pm 0.1) \mu s$  and  $\tau_{decay} = (41.6 \pm 0.1) \mu s$ .

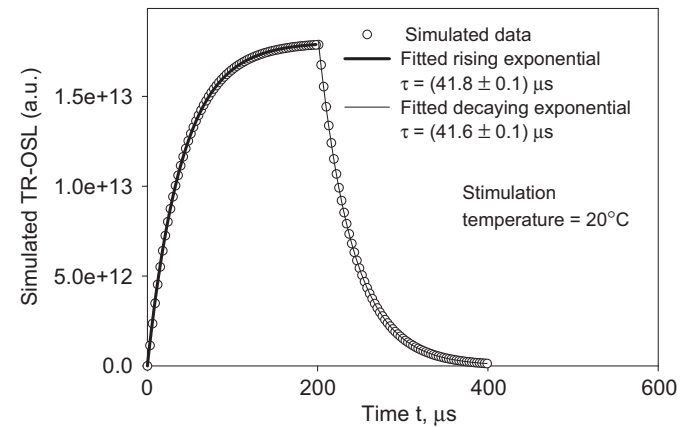
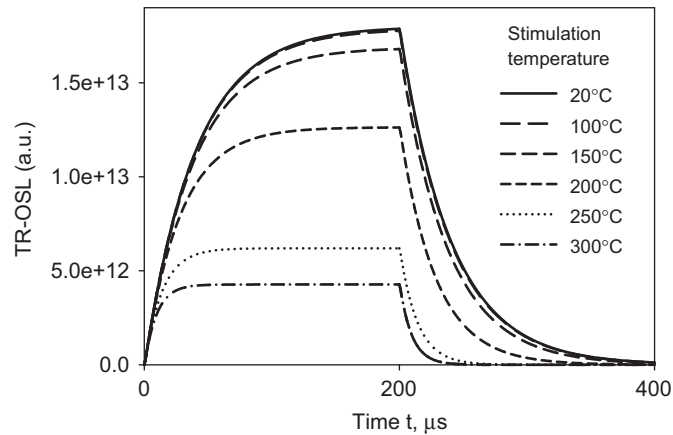


Fig. 2. Simulated time resolved spectrum for quartz using the model shown in Fig. 1. The LED stimulation is ON for 200  $\mu s$  and OFF for the same amount of time. The rising and decaying parts of the signal are fitted with a rising exponential and a decaying exponential correspondingly.

We have repeated this simulation by varying the stimulation temperature in the range 20–300 °C, with the results shown in Figs. 3 and 4. It is noted that the preheat and irradiation parts of



**Fig. 3.** Simulated time resolved spectra for quartz at various stimulation temperatures between 20 and 300 °C. As the stimulation temperature increases the corresponding luminescence lifetime decreases for both parts of the signal.

the experimental procedure are not part of the simulation, but we assume instead a non-zero initial concentration of electrons in the dosimetric trap, as was explained in the previous section. Fig. 3 shows clearly that as the stimulation temperature increases, the luminescence lifetime for both the rising and falling part of the signal decrease continuously because of thermal quenching. The luminescence lifetimes  $\tau$ , obtained by fitting single exponentials to the simulated TR-OSL curves in Fig. 3, are shown in Fig. 4. The simulation results in Fig. 4a show that as the stimulation temperature increases, the luminescence lifetimes obtained from the exponential fits decrease smoothly from  $\sim 42 \mu\text{s}$  to  $\sim 2 \mu\text{s}$  in the temperature range 20–300 °C. It is noted that the rising and decaying parts of all simulated TR-OSL signals in Fig. 3 yield indistinguishable luminescence lifetimes, in agreement with the results of several previous experimental studies ([19]). Because we have chosen parameter values such that the conduction band empties much faster than the excited state of the recombination center, we see no evidence for the presence of multiple exponential components in these simulations.

Superimposed on the simulated data of Fig. 4a we show the experimental data on the luminescence lifetime  $\tau$  for sample WIDG8 (open triangles), including recycling points at 40, 100, 200

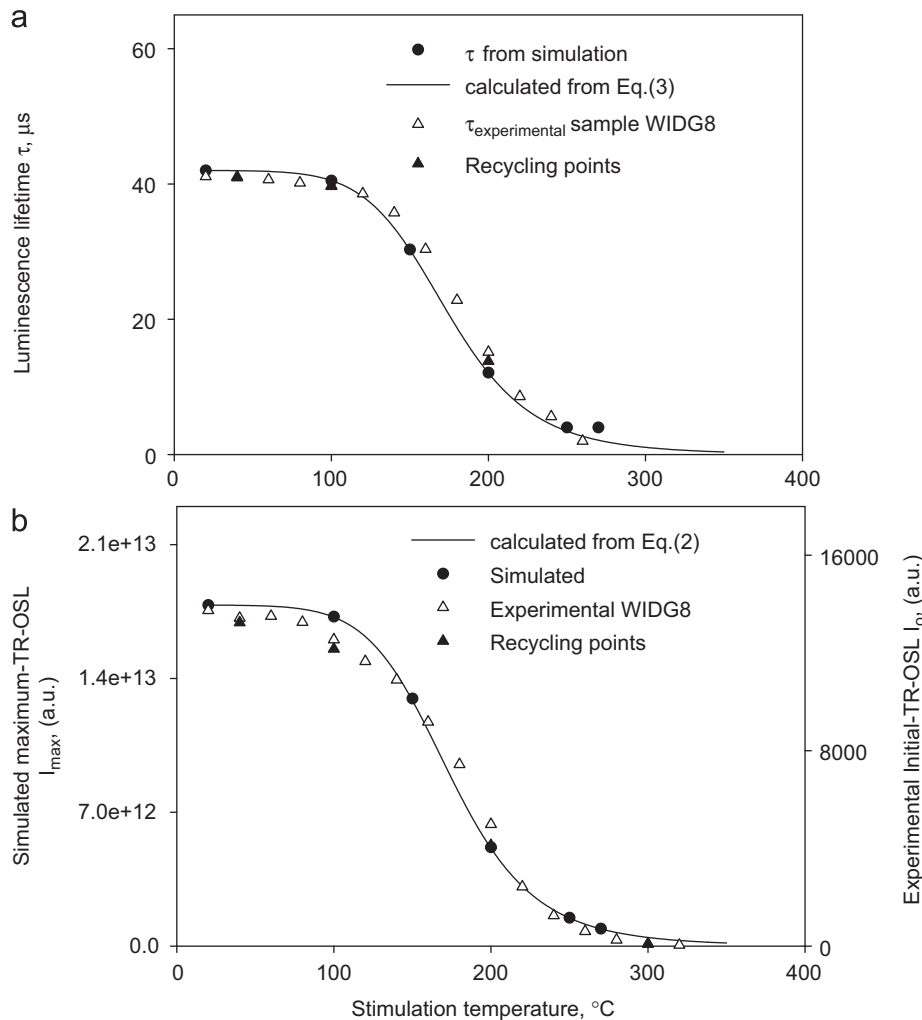


**Fig. 4.** (a) Experimental dependence of the luminescence lifetime  $\tau$  on the stimulation temperature for sample WIDG8 is shown as the open triangles and filled triangles denote recycling points. The solid line indicates the best fits to the simulated data using the thermal quenching Eq. (4) with an activation energy  $W=0.64 \text{ eV}$  and the dimensionless constant  $C=1.64 \times 10^7$ . The solid circles show the simulated luminescence lifetimes obtained from Fig. 3 and (b) The experimental dependence of the maximum luminescence intensity on the stimulation temperature for sample WIDG8 is shown by the open triangles and recycling points as filled triangles. The solid line is calculated using the thermal quenching Eq. (3). The solid circles show the maximum luminescence intensity obtained from the simulated TR-OSL spectra in Fig. 3.

and 300 °C (filled triangles). The solid line in Fig. 4a indicates the best fit to the simulation data using the thermal quenching equation (3) with an activation energy  $W=0.64$  eV and a value of the non-radiative probability  $A_{NR}=3.9 \times 10^{11} s^{-1}$ , corresponding to a value of the dimensionless constant  $C=A_{NR}/A_R=1.64 \times 10^7$ .

Fig. 4b shows the maximum TR-OSL intensity of the simulated signals shown in Fig. 3, as a function of the stimulating temperature. Superimposed on the simulated data we show the corresponding experimental data for sample WIDG8, as well as the calculated maximum intensity using equation (2). The solid line in Fig. 4b indicates the best fit to the simulated data using the thermal quenching equation (3), and with the same parameters C, W used in Fig. 4a.

The simulation data in Fig. 5 show typical examples of the time variation of the concentrations of electrons in the CB and in the excited state ( $n_2$ ) during the decaying signal of the TR-OSL experiment at room temperature. As expected from our choice of parameters, the lifetimes of electrons in the CB are extremely short as compared with the lifetime in the excited state. With the choice of parameters in the model the CB empties very quickly within a few  $\mu s$  as shown in the inset of Fig. 5, while the excited state decays radiatively much slower in agreement with the

experimentally observed lifetime of  $\sim 40 \mu s$  at room temperature. The corresponding TR-OSL signal decays at the exact same rate as the excited state ( $n_2$ ), in agreement with equation (7).

### 6. Further results of the model

During a typical TR-OSL experiment, the signals from several thousands of pulses are added digitally to yield the measured total luminescence signal. An important consideration during such experiments is whether the shape of the individual TR-OSL spectra stays the same between pulses, and therefore whether one can justifiably add many individual pulses. We have simulated such a sequence of 100,000 pulses using the model of Fig. 1, with the concentrations at the end of each pulse being used as the initial concentrations of the next pulse. The resulting TR-OSL signals in this simulation are shown in Fig. 6, where it is seen that even after 100,000 pulses the TR-OSL signal maintains its shape and yields the same luminescence lifetime. The results of the simulation show that after 100,000 pulses the concentration of holes in the recombination center decreases by only 3.5% of its initial value.

An important result from the model is that it produces reasonable results for very long illumination times of the order of seconds. In such a case one expects that the results of the simulation would resemble what is seen experimentally during a continuous-wave (CW-OSL) experiment. In this simulation of long

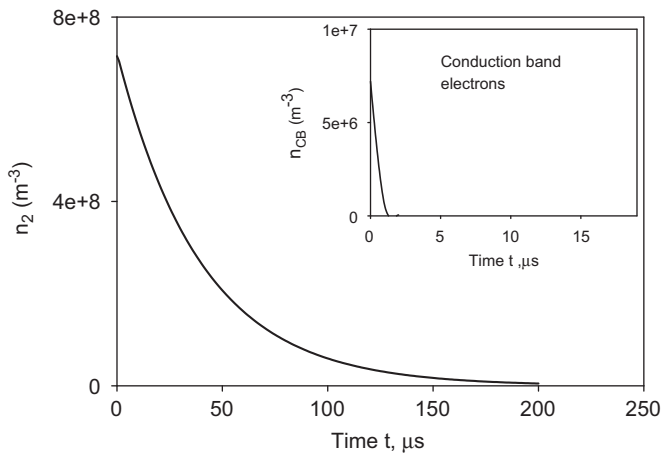


Fig. 5. (a) The variation of the electron concentration  $n_2$  in the excited state of the recombination center (level 2 in Fig. 1b), as a function of time during the decaying OFF-time period of the TR-OSL signal at room temperature. The luminescence lifetime of electrons in the CB is very short as seen in the inset, while the lifetime of the excited state ( $n_2$ ) is much longer. (b) The observed TR-OSL signal decays at exactly the same rate as the concentration of electrons in the excited state, as shown in (a).

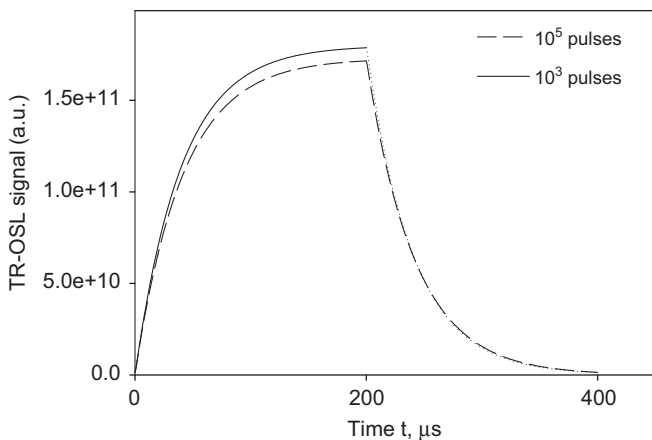


Fig. 6. Simulation of the TR-OSL signals after summation of 1,000 pulses and after summation of 100,000 pulses.

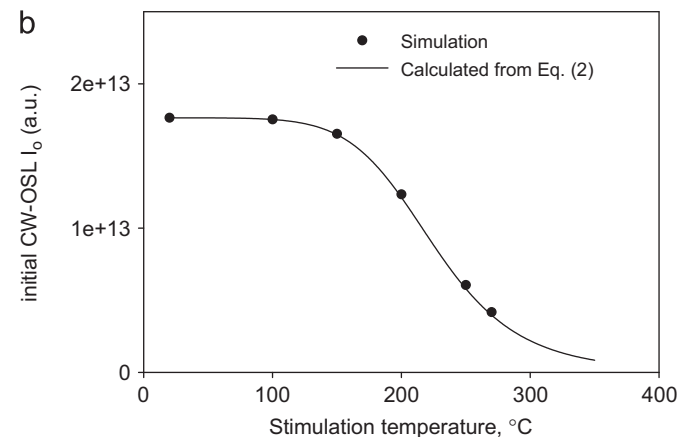
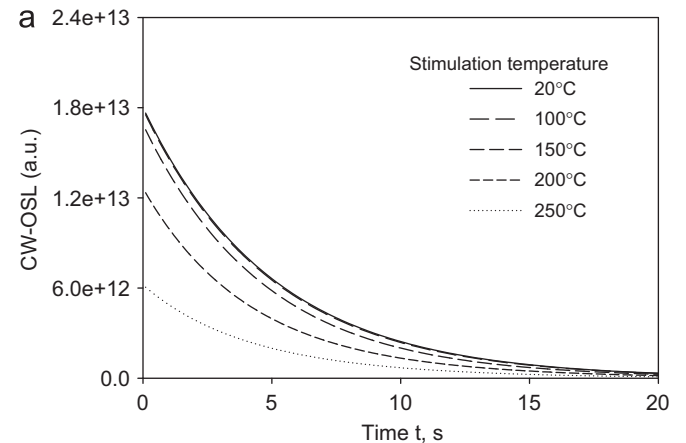
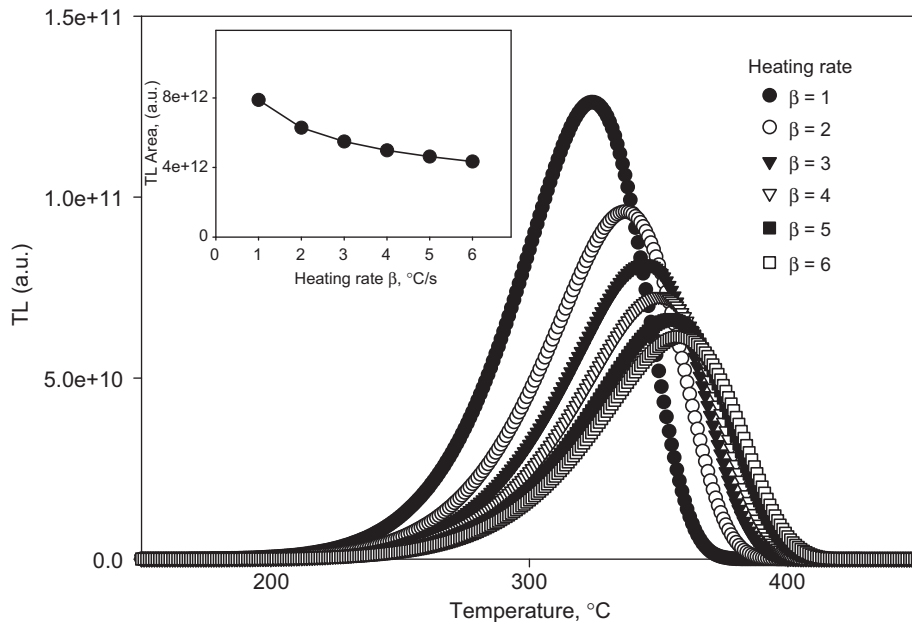


Fig. 7. (a) Simulation of the TR-OSL signal when the optical stimulation is ON for very long times, while the OFF period is not important in this type of simulation. The resulting curves are similar to “shine down” curves obtained experimentally during a continuous-wave CW-OSL experiment (b) variation of the area under the shine down curves in (a), with the stimulation temperature (solid circles). The solid line is calculated using Eq. (3) for thermal quenching.



**Fig. 8.** Simulation of the thermoluminescence (TL) signal measured with different heating rates, by using the model in Fig. 1. The inset shows the variation of the area under the TL glow curves as function of the heating rate. The simulated decrease of the TL area with the heating rate is due to the presence of thermal quenching.

illumination times, the optical stimulation is left ON for a time period of several seconds, while the OFF part of the simulation is not important in this type of simulation. As seen in Fig. 7a, the resulting signal is very similar to an OSL decay curve measured during a CW-OSL experiment. The simulation was repeated for different simulation temperatures and the results are shown in Fig. 7a. Fig. 7b shows the area under the stimulation curves in Fig. 7a as a function of the stimulation temperature, together with the results from Eq. (3), showing good agreement between the results of the simulation and the thermal quenching factor.

A third important result of the model is that it reproduces the well-known decrease in the thermoluminescence (TL) signal due to thermal quenching. Specifically when TL glow curves are measured using a variable heating rate, the TL intensity is found to decrease as the heating rate increases. The result of simulating the TL glow curves using different heating rates is shown in Fig. 8, using typical kinetic parameters for the 325 °C TL peak of quartz (activation energy  $E=1.65$  eV and frequency factor  $s=10^{12}$  s $^{-1}$ ). As the heating rate increases, the TL glow peaks become wider and shift towards higher temperatures, while their intensity decreases significantly. The inset to Fig. 8 shows the decrease of the total area under the TL glow curves with the heating rate, a well-known experimental effect due to thermal quenching.

## 7. Discussion

Several experimental studies of quartz samples have elucidated the nature of the recombination centers in quartz. It is believed that the main quartz emission band at 380 nm is due to recombination processes taking place at  $(H_3O_4)^0$  hole centers ([24]). Furthermore, it is thought that the 110 °C TL signal and at least part of the main OSL signal from quartz are also associated with this hole center. Additional quartz emission bands have been identified at 420 nm ([25]) and at 460 nm, with the latter emission believed to be due to  $(AlO_4)^0$  centers ([24]). Later experimental studies have provided important links between specific impurities in quartz and ionic movements in the crystal, as well as additional information on the nature of the ionic

complexes involved in the luminescence process in quartz ([26–29]).

In the rest of this section we discuss the relationship between the quartz model presented in this paper and the more comprehensive quartz models found in the literature ([6,30,31]). For comparison purposes we choose the model of Bailey [6] as a representative example of commonly used phenomenological quartz models. The purpose of this discussion is to emphasize the differences between localized and delocalized transitions contained in the models. The Bailey model contains a total of 5 electronic levels and 4 hole centers, and has been used successfully to simulate a wide variety of TL and OSL experiments in quartz. In this model the luminescence intensity from quartz is written as (Bailey, [6], p.22, Eq. (6)):

$$I(t) = A_{CB} m n_c \eta(T), \quad (8)$$

where  $A_{CB}$  represents the probability of electronic transitions from the conduction band into the recombination center,  $m$  represents the instantaneous concentration of holes in the recombination center,  $n_c$  the concentration of electrons in the CB, and  $\eta(T)$  is the “luminescence efficiency factor” given by a Mott-Seitz type of expression

$$\eta(T) = \frac{1}{1 + C \exp(-W/k_B T)}. \quad (9)$$

Within the Bailey model, Eq. (8) above clearly represents mathematically a *delocalized* transition involving electrons in the conduction band. Furthermore, Eq. (9) above in the Bailey model expresses mathematically the thermal quenching process by using a phenomenological efficiency factor  $\eta(T)$ .

By contrast, in the model presented in this paper the luminescence intensity is expressed by the expression

$$I(t) = A_R n_2, \quad (10)$$

which represents mathematically a *localized* transition from the excited level of the recombination center into the ground state of the same center. In the model of Fig. 2, all transitions are of a localized nature, except for transition 3 which involves electrons in the CB and hence is delocalized. Mathematically this

delocalized transition is expressed by the term  $A_{CB}n_c(N_2 - n_2)$  in Eqs. (5) and (6). The present model is therefore a mathematical description of a completely internal mechanism within the recombination center, and is based on electronic transitions of a localized nature. Furthermore, the present model is developed in terms of electrons occupying multiple energy states within the recombination center, while in the Bailey delocalized model one considers a single radiative transition from the CB into the recombination center.

We have attempted to simulate the TR-OSL experiment described in this paper using the Bailey (2001) model, and found that the relaxation time within the model is  $\tau \sim 0.1$  s, three orders of magnitude larger than the experimentally found value of  $\tau = 42 \mu\text{s}$ . It is possible to select parameter values within the Bailey model that will give a lifetime consistent with experiment, and also with the experimentally observed decrease in luminescence intensity with stimulation temperature. However, in the Bailey and other similar models there is no process by which this lifetime is temperature dependent, in contrast to experimental observation and the predictions of our model.

The ultimate goal of a comprehensive thermal quenching model for quartz should be a more inclusive model, namely a model which would combine the delocalized processes in the Bailey model with an appropriate modification of the parameter values to explain observed emptying of the conduction band from the TR-OSL experiments, and the localized processes described in this paper. Such a comprehensive model would be able to describe a wider variety of luminescence phenomena in quartz, from a time scale of microseconds to tens of seconds. Such an encompassing effort is currently in progress.

## 8. Conclusions

The Mott–Seitz mechanism for thermal quenching in quartz was first suggested several decades ago, and provides a physical explanation based on localized transitions for several thermal quenching phenomena in quartz. In this paper we presented a simple kinetic model for the Mott–Seitz mechanism. The model provides a satisfactory mathematical description of the internal thermal quenching mechanism of luminescence in quartz. The results of the model compare quantitatively with new experimental results obtained using a single aliquot procedure on a sedimentary quartz sample.

The model can be applied to several types of luminescence experiments involving very different time scales. In the case of TR-OSL experiments the model can describe thermal quenching phenomena within a time scale of microseconds, while in the case of CW-OSL and TL experiments the model provides a satisfactory description of the thermal quenching kinetics within a time scale of tens of seconds.

One important conclusion from the model presented here, is that the existing model parameters for quartz do not allow quick enough emptying of the CB, and therefore cannot explain

the TR-OSL data. Specifically, all available experimental evidence points that no matter what the quartz type, the TR-OSL lifetime at room temperature should be of the order of tens of  $\mu\text{s}$ . However, as pointed out above, the relaxation time within the Bailey model is  $\tau \sim 0.1$  s, three orders of magnitude larger than the experimental value. This is of course not a fundamental failure in the current models, but rather it calls for a re-evaluation of the available model parameters for quartz.

## Acknowledgements

The financial support provided by the Luminescence Laboratory for Nordic Studies and by Risø-DTU is gratefully acknowledged by V. Pagonis. We thank Prof. R. Roberts, for providing and preparing the sedimentary quartz (sample WIDG8; Ref. [20]).

## References

- [1] L. Bøtter-Jensen, S.W.S. McKeever, A.G. Wintle, in: *Optically Stimulated Luminescence Dosimetry*, Elsevier, Amsterdam, 2003.
- [2] A.G. Wintle, *Geophys. J. R. Astron. Soc.* 41 (1975) 107.
- [3] B.W. Smith, E.J. Rhodes, S. Stokes, N.A. Spooner, *Rad. Prot. Dosim.* 34 (1990) 75.
- [4] N.A. Spooner, *Radiat. Meas.* 23 (1994) 593.
- [5] R. Chen, S.W.S., McKeever, 1997. *Theory of Thermoluminescence and Related Materials* (World Scientific).
- [6] R.M. Bailey, *Radiat. Meas.* 33 (2001) 17.
- [7] G. Kitis, *Phys. Status Solidi (A)*, Appl. Res. 191 (2002) 621.
- [8] D.C.W. Sanderson, R.J. Clark, *Radiat. Meas.* 23 (1994) 633.
- [9] I.K. Bailiff, *Radiat. Meas.* 32 (2000) 401.
- [10] S. Tsukamoto, P.M. Denby, A.S. Murray, L. Bøtter-Jensen, *Radiat. Meas.* 41 (2006) 790.
- [11] P.M. Denby, L. Bøtter-Jensen, A.S. Murray, K.J. Thomsen, P. Moska, *Radiat. Meas.* 41 (2006) 774.
- [12] M.L. Chithambo, F.O. Ogundare, J. Feathers, *Radiat. Meas.* 43 (2008) 1.
- [13] C. Ankjærgaard, M. Jain, R. Kalchgruber, T. Lapp, D. Klein, S.W.S. McKeever, A.S. Murray, P. Morthekeai, *Radiat. Meas.* 44 (2009) 576.
- [14] V. Pagonis, S.M. Mian, M.L. Chithambo, E. Christensen, C. Barnold, *J. Phys. D: Appl. Phys.* 42 (2009) 055407.
- [15] R.B. Galloway, *Radiat. Meas.* 35 (2002) 67.
- [16] M.L. Chithambo, *Radiat. Meas.* 37 (2003) 167.
- [17] M.L. Chithambo, *Radiat. Meas.* 41 (2006) 862.
- [18] M.L. Chithambo, *J. Phys. D: Appl. Phys.* 40 (2007) 1874.
- [19] M.L. Chithambo, *J. Phys. D: Appl. Phys.* 40 (2007) 1880.
- [20] A.G. Wintle, A.S. Murray, *Radiat. Meas.* 27 (1997) 611.
- [21] T. Lapp, M. Jain, C. Ankjærgaard, L. Pirzel, *Radiat. Meas.* (2009), available online as doi:10.1016/j.radmeas.2009.01.012.
- [22] D. Curie, in: *Luminescence in Crystals*, Wiley, New York, 1963.
- [23] N.F. Mott, R.W. Gurney, in: *Electronic Processes in Ionic Crystals*, 2nd ed., Oxford University Press, London, 1948.
- [24] X.H. Yang, S.W.S. McKeever, *J. Phys. D: Appl. Phys.* 23 (1990) 237.
- [25] I.K. Bailiff, *Radiat. Meas.* 23 (1994) 471.
- [26] N. Itoh, D. Stoneham, A.M.J. Stoneham, *Phys. Condens. Matter* 13 (2001) 2201.
- [27] T. Schilles, N.R.J. Poolton, E. Bulur, L. Bøtter-Jensen, A.S. Murray, G.M. Smith, P.C. Riedi, G.A. Wagner, *J. Phys. D: Appl. Phys.* 34 (2001) 722.
- [28] N.R.J. Poolton, G.M. Smith, P.C. Riedi, E. Bulur, L. Bøtter-Jensen, A.S. Murray, M. Adrian, *J. Phys. D: Appl. Phys.* 33 (2000) 1007.
- [29] E. Vartanian, P. Guibert, C. Roque, F. Bechtel, M. Schvoerer, *Radiat. Meas.* 32 (2000) 647.
- [30] G. Adamiec, *Radiat. Meas.* 39 (2005) 175.
- [31] V. Pagonis, A.G. Wintle, R. Chen, X.L. Wang, *Radiat. Meas.* 43 (2008) 704.